An apoA-I mimetic peptide containing a proline residue has greater in vivo HDL binding and anti-inflammatory ability than the 4F peptide

Geoffrey D. Wool,* Tomas Vaisar,† Catherine A. Reardon,* and Godfrey S. Getz*,[1]

Department of Pathology,* University of Chicago, Chicago, IL; and Department of Medicine,† University of Washington, Seattle, WA

Abstract **Modifying apolipoprotein (apo) A-I mimetic peptides to include a proline-punctuated α-helical repeat increases their anti-inflammatory properties as well as allows better mimicry of full-length apoA-I function. This study compares the following mimetics, either acetylated or biotinylated (b): 4F (18mer) and 4F-proline-4F (37mer, Pro). b4F interacts with both mouse HDL (moHDL) and LDL in vitro. b4F in vivo plasma clearance kinetics are not affected by mouse HDL level. Administration of biotinylated peptides to mice demonstrates that b4F does not associate with lipoproteins smaller than LDL in vivo, though it does associate with fractions containing free hemoglobin (Hb). In contrast, bPro specifically interacts with HDL. b4F and bPro show opposite binding responses to HDL by surface plasmon resonance. Administration of acetylated Pro to apoE$^{-/-}$ mice significantly decreases plasma serum amyloid A levels, while acetylated 4F does not have this ability. In contrast to previous reports that inferred that 4F associates with HDL in vivo, we systematically examined this potential interaction and demonstrated that b4F does not interact with HDL in vivo but rather elutes with Hb-containing plasma fractions. bPro, however, specifically binds to moHDL in vivo. In addition, the number of amphipathic α-helices and their linker influences the anti-inflammatory effects of apoA-I mimetic peptides in vivo.**—Wool, G. D., T. Vaisar, C. A. Reardon, and G. S. Getz. **An apoA-I mimetic peptide containing a proline residue has greater in vivo HDL binding and anti-inflammatory ability than the 4F peptide.** ***J. Lipid Res.*** **2009.** 50: **1889–1900**.

Supplementary key words apolipoprotein A-I • high density lipoprotein • synthetic peptides • cholesterol • inflammation • oxidation

Apolipoprotein (apo) A-I mimetic peptides have been shown to have notable anti-inflammatory and antiatherosclerotic properties and have much promise as potential therapeutic agents for atherosclerosis-related diseases. A good deal of attention has been devoted to crafting an "ideal" mimetic peptide (1, 2). This includes the comparison of single and tandem mimetic peptides. Aside from our prior study (3), almost all previous studies of tandem mimetic peptides have involved tandems based upon 18A (2F) rather than the 4F peptide, the monomeric mimetic peptide most extensively studied for its antiatherogenic potential.

We have previously demonstrated that tandem 4F-based peptides have different in vitro properties than monomeric 4F. The proline-punctuated tandem peptide (4F-proline-4F, Pro) exceeds 4F in its HDL remodeling potency as well as ability to efflux cholesterol from cultured foam cells. On the other hand, 4F had more antioxidative ability than Pro (3).

In the current study, we demonstrate the lipoprotein-association profile and the short-term in vivo behavior of selected single and tandem 4F-based peptides. We hypothesize that apoA-I mimetic peptide structure influences lipoprotein-association properties, thereby modifying peptide plasma kinetics as well as therapeutic efficacy. A proline residue in a right-handed α-helix has been shown to cause a kink of ~23° in the helix axis (4). α-Helices themselves can adopt a curvature of ~1° of arc per residue (5). Therefore, the maximum possible deviation from a perfectly straight helical rod expected for the Pro peptide (37 amino acids) is ~60°. Based on that prediction, the Pro

This work was supported by NHLBI (HL68661) and the LeDucq Foundation. G.D.W. has received support from NICHHD (HD007009 Graduate Training in Growth and Development), Francis L. Lederer Foundation Scholarship Fund, and an American Heart Association predoctoral fellowship.

Manuscript received 1 April 2009 and in revised form 8 May 2009.

Published, JLR Papers in Press, May 11, 2009
DOI 10.1194/jlr.M900151-JLR200

Abbreviations: apo, apolipoprotein; AUC, area under the curve; b4F, biotinylated 4F; bPro, biotinylated Pro; DMF, dimethylformamide; ECL, enhanced chemiluminescence; FPLC, fast protein liquid chromatography; Hb, hemoglobin; HDL-C, HDL cholesterol; HRP, horseradish peroxidase; huHDL, human HDL; IP, intraperitoneal; MDA, malondialdehyde; moHDL, mouse HDL; moLDL, mouse LDL; Pro, 4F-proline-4F; RU, response unit; SAA, serum amyloid A; SPR, surface plasmon resonance; TBARS, thiobarbituric acid-reactive substance; TC, total cholesterol; TEP, 1,1,3,3-tetraethoxypropane.

[1] To whom correspondence should be addressed.
e-mail: g-getz@uchicago.edu

peptide will likely preferentially associate with lipoproteins that possess a small radius of curvature (i.e. HDL). Using the same principles, the maximum possible deviation from a straight helical rod expected for the 18mer 4F peptide is 18°. Given the short sequence of 4F and the resulting deficit of potential curvature, we hypothesize that the 4F peptide will associate with lipoproteins more like a straight rod and will be more able to interact with a broader range of lipoproteins. However, given data in the literature, 4F likely still prefers HDL. Previous studies with 18A in rats have shown the peptide to be almost completely HDL associated (6), while 5F administration to mice resulted in both VLDL and HDL association (7).

After having defined the plasma clearance and lipoprotein-association behavior of biotinylated peptides, we also investigated the effect of short-term treatment of apoE$^{-/-}$ mice with acetylated peptides. Combining the results of lipoprotein-association studies with short-term treatment studies provides improved understanding of the potential mechanism of action of the peptides in vivo.

METHODS

Peptides

Peptides were either synthesized from L-amino acids and purified as described (3) or purified peptides were purchased from BioSynthesis (Lewisville, TX). All peptides were modified at their N termini (biotinylation for tracking, or acetylation) and C termini (amidation). The acetylation and amidation of apoA-I mimetic peptides have been shown to increase many of the apoA-I mimicking properties of the peptide (8). We adhere to the standard used by previous reports and reviews in the apoA-I mimetic peptide literature that the denomination "4F" denominates the following peptide: Ac-DWFKAFYDKVAEKFKEAF-NH2 (2).

N-terminal peptide biotinylation was carried out according to the protocol of Anaspec Corp.. (San Jose, CA). Briefly, 244 mg unmodified (+)-biotin (Sigma) was solubilized in 2 ml dimethylsulfoxide to which was added 1 ml dimethylformamide (DMF), 2 ml 0.5M 2-(1*H*-benzotriazole-1-yl)-1,1,3,3-tetramethyluronium hexafluorophosphate in DMF, and 452 µl diisopropylethylamine, sequentially. This solution was added to the peptide-containing uncleaved resin serially for room temperature stirring until the coupling was complete by qualitative ninhydrin assay.

N-terminal peptide acetylation was carried out according to the protocol of Anaspec Corp. (San Jose, CA). Briefly, 10% acetic anhydride in DMF was added to the peptide-containing uncleaved resin in 10 ml aliquots serially until the coupling was complete by qualitative ninhydrin assay.

After trifluoroacetic acid cleavage, peptides were purified by reverse phase-HPLC on a preparative C18 column using water-acetonitrile gradients in 0.1% v/v trifluoracetic acid at a flow rate of 10 ml/min. Purity was confirmed by analytical reverse phase-HPLC. Alternatively, peptides were ordered at >90% purity from BioSynthesis.

Peptides administered to mice were solubilized in sterile PBS.

Mice

All mice were in the C57BL/6 genetic background and were bred in-house. They were housed in micro-isolators in a specific pathogen-free barrier facility at the University of Chicago and experimental procedures performed in accordance with National Institutes of Health guidelines under protocols approved by the Institutional Animal Care and Use Committee.

Wild-type C57BL6, apoE$^{-/-}$, and apoA-I$^{-/-}$/apoE$^{-/-}$ mice were maintained on a standard laboratory chow diet (6.25% fat, Harlan Teklad TD7913). Mice receiving intraperitoneal (IP) injections received antibiotic-treated (trimethoprim/sulfamethoxazole) acidified drinking water throughout the course of the experiment.

At 7-8 weeks of age, the mice were bled from their retro-orbital plexus after at least a 4 h fast and their plasma total cholesterol (TC) level was determined. apoE$^{-/-}$ mice were used for various studies depending on their TC level: short-term peptide injection studies (250–450 mg/dl TC) or biotinylated peptide clearance studies (<500 mg/dl TC). apoA-I$^{-/-}$/apoE$^{-/-}$ mice used in the biotinylated peptide clearance study had TC levels <500 mg/dl.

Mice in peptide clearance or lipoprotein association studies were injected IP with 300 µg biotinylated 4F (b4F) or biotinylated Pro (bPro) solubilized in ~500 µl sterile PBS. Mice were provided with standard chow during the course of the experiment. The mice were bled retro-orbitally at selected time points into EDTA-coated microtainers.

Mice undergoing short-term peptide injection received three total IP injections over the course of 1 week starting at 8–12 weeks of age. Peptides were brought up in sterile PBS and not filter sterilized. A group of mice receiving filter-sterilized 4F showed no significant differences to unfiltered 4F in any parameter (data not shown). The mice were injected every other day with 50 µg L4F, 100 µg tandem peptide, or PBS control; the total injection volume was 200 µl PBS. This translates as ~1.25 µg L4F peptide/g mouse/day or ~2.5 µg tandem peptide/g mouse/day, i.e. equal molar concentrations. All mice were euthanized 2 h after the concomitant last peptide injection.

Lipoproteins

Mouse lipoproteins were isolated by sequential ultracentrifugation of pooled plasma from mice with wild-type apolipoprotein genotypes. Mouse or human LDL was isolated between a density of 1.019 and 1.063 g/ml and mouse HDL (moHDL) between a density of 1.063 and 1.21 g/ml. Lipoprotein distribution in mouse plasma was analyzed by either equilibrium density ultracentrifugation (9) or fast protein liquid chromatography (FPLC) (10). Cholesterol was measured using Roche (Indianapolis, IN) enzymatic assay and protein by Bio-Rad (Hercules, CA) protein assay (500-0006), all according to the manufacturer's protocol. Lipoprotein distribution was determined by area under the curve (AUC) analysis of the fractional TC data. Fractions were grouped as chylomicron remnant/VLDL, LDL, or HDL.

Electrophoresis and immunoblotting

Gradient SDS-PAGE gels were formed per Bio-Rad Mini-PROTEAN 3 manual instructions. Agarose electrophoresis was carried out in 0.7% agarose gels in 25 mM tricine/3 mM calcium lactate (pH 8.6) buffer. For immunoblotting, agarose gels and SDS-PAGE gels were transferred to Immobilon (Millipore, Bedford, MA) for 1 h at 400 mA. The following antibodies were used for primary immunoblotting: polyclonal rabbit anti-mouse apoA-I, polyclonal rabbit anti-mouse serum amyloid A (SAA), and polyclonal rabbit anti-mouse hemoglobin (Hb) (MP Biosciences no. 55447). Affinity purified horseradish peroxidase (HRP)-linked polyclonal goat anti-rabbit IgG (Sigma, St. Louis, MO; A-4914) was used for the secondary probe. Membranes were visualized by enhanced chemiluminescence (ECL) and images captured using AlphaImager (AlphaInnotech, San Leandro, CA). Blots were quantitated using the spot densitometry feature of the FluoroChem v2.0 program.

Biotinylated peptide clearance/lipoprotein association assays

Dilute plasma, ultracentrifugation fractions, or FPLC fractions were applied to Immobilon membrane in a Schleicher and Schuell (Keene, NH) Minifold II slot blot apparatus. 0–0.1 μg low-range SDS-PAGE biotinylated protein standards (Bio-Rad) provided an ECL signal standard curve. The membrane was probed with streptavidin-HRP (Jackson ImmunoResearch 016-030-084) at 0.5 μg/ml. Blots were exposed with ECL solution, images captured on an AlphaImager, and signals quantified as described above.

For assays of plasma clearance of biotinylated peptide, the ECL signal from the 0 h bleed (before peptide injection) was subtracted from all time points to normalize for the preexisting biotin concentration in mouse plasma. After that normalization, AUC analysis was carried out. For assays of FPLC fractions, each treated mouse was paired with a control PBS-treated mouse and the biotin peptide-specific signal was determined by subtraction.

Surface plasmon resonance assay

The affinity and rates of interaction of b4F and bPro for mouse HDL (moHDL) or human HDL (huLDL) were measured by surface plasmon resonance (SPR) on a BIAcore 3000 biosensor. Peptides were bound to the dextran matrix of a sensor chip by streptavidin (Sensor Chip SA no. BR-1003-98). Kinetic experiments were performed at 25°C in HBS-N (10 mM HEPES, pH 7.4, 0.15 M NaCl, 50 μM EDTA, without Tween). Analytes were added at various concentrations and the amount of protein bound to the chip was monitored by the change in refractive index [response units (RU)]. After the completion of analyte injection, an equal time of buffer injection allowed determination of analyte dissociation behavior. The analytes were assumed to have the following particle weights: moHDL, 300,000 (11); huLDL, 3,500,000 (12).

Serum analysis

The paraoxonase activity assay was modified from that of Cabana et al. (13). A total of 25.5 μl mouse serum was diluted to 1 ml in PON buffer (10 mM Tris/1 mM $CaCl_2$, pH 8.0). A total of 0–160 μl of dilute serum was brought up to 900 μl in PON buffer and 100 μl of 10 mM phenyl acetate (in PON buffer) was added. The OD270 change/min for each serum concentration in triplicate created a linear dose-response curve whose slope defined the serum PON arylesterase activity. The slope was converted to PON arylesterase units (U in mol/l): $(\Delta OD/min/ml)/(1310\ M^{-1}\ cm^{-1})$.

The plasma thiobarbituric acid-reactive substances (TBARS) assay was modified from that of Lapenna et al. (14) and Aviram et al. (15). A total of 30 μl mouse plasma or 0–0.55 μg of 1,1,3,3-tetraethoxypropane (TEP) (Sigma) as an malondialdehyde (MDA)-precursor standard were brought up to 200 μl. An equal volume of TBARS reagent (0.375% 2-thiobarbituric acid, 15% trichloroacetic acid, 1% SDS, 2.5 mM butylated hydroxytoluene, 0.25N HCl) was added and heated at 95°C for 30 min. The reaction was removed from heat, cooled at 4°C, centrifuged at 2000 rpm for 3 min in a benchtop microcentrifuge, and the supernatant removed. An equal volume of butanol was added to the supernatant and the solution was mixed. The solution was centrifuged at 2000 rpm for 3 min in a benchtop microcentrifuge and the optical absorbance of the supernatant was measured as the difference between OD532 and OD572. Plasma TBARS reactivity was converted into TEP equivalents based upon the linear standard curve. All TBARS reactivity assays were performed the same day as plasma isolation.

Statistics

Data are presented as average ± SD. Data processing and statistical analyses were performed by Microsoft Excel using the Student's *t*-test for significant differences.

RESULTS

b4F in vivo clearance is not affected by moHDL status

Plasma clearance and lipoprotein-association experiments delineated here require the ability to track peptide. No antibody against 4F peptides is currently available. Previous reports that have tracked 4F have used the fluorescent tag N-methyl-*O*-aminobenzoic acid (N-methyl anthranilyl) (2). We have used N-terminal peptide biotinylation and tracked peptides with avidin probes. The uncharged biotin moiety is connected to the N terminus of the peptide through an uncharged amide bond. Biotinylation of the peptide does not alter the amphipathicity of the helix residues themselves, as would be the case with radiolabeling by tyrosine iodination. Also, most of the tracking experiments described below are head-to-head comparisons of the differences between two biotinylated peptides: bPro and b4F. By comparing the behavior of two peptides with the same modification, the influence of the biotin modification is minimized.

Previous reports showed that the peptides 18A, D4F, and 5F specifically associate with rodent HDL in vivo (2, 6, 7). Given this finding, we hypothesized that the plasma clearance of b4F would be influenced by mouse plasma HDL status. We compared the clearance of b4F in wild-type C57BL/6, $apoE^{-/-}$, and $apoE^{-/-}$apoA-$I^{-/-}$ mice. Average plasma TC (mg/dl) in these mice was 70 (C57), 368 (EA), 526 (E), while average plasma HDL cholesterol (HDL-C) (mg/dl) was <5 (EA), 18 (E), 70 (C57) [(16); data not shown). Each mouse was injected IP with 300 μg b4F and the kinetics of peptide plasma clearance were monitored.

Peptide signal appeared in the plasma quickly, within 0.5–1.5 h (**Fig. 1A**), with maximal plasma concentration achieved within 3–5 h. The $t_{1/2}$ of IP-administered b4F was <24 h for all mouse strains. AUC analysis of plasma clearance curves demonstrated no significant differences in total plasma b4F regardless of moHDL status (Fig. 1B). If anything, b4F achieved higher plasma concentrations in $apoE^{-/-}$ mice. Thus, peptide plasma clearance did not follow HDL status and showed a trend toward greater plasma concentration in the mouse model with the highest plasma TC. This result suggested that b4F may associate with non-HDL lipoproteins in vivo.

b4F interacts with moHDL and LDL in vitro

To shed light on the basis of this unexpected finding that HDL levels do not influence b4F clearance, we investigated the lipoprotein-association behavior of b4F in vitro. b4F was equilibrated with isolated lipoprotein populations and the mixture was separated by ultracentrifugation on density gradients. The gradient fractions were analyzed by slot blot with avidin-HRP.

When incubated with mouse LDL (moLDL), b4F showed a broad, strong signal peak that colocalized with LDL as determined by the cholesterol content of the fractions (**Fig. 2**). When incubated with moHDL, b4F also showed robust association with that lipoprotein. The presence of HDL in the density gradient fractions was assessed

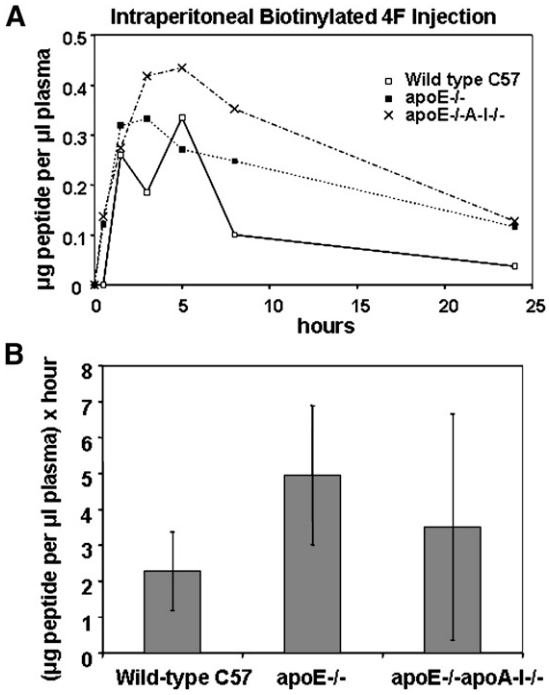

Fig. 1. IP administration of b4F peptide to mice. Wild-type, apoE$^{-/-}$, and apoE$^{-/-}$apoA-I$^{-/-}$ mice were injected IP with 300 µg b4F and ~100 µl of blood was removed at the indicated time points. Dilute plasma was applied to Immobilon in a slot-blot apparatus and the membrane was probed with avidin-HRP to detect the peptide. The blot was quantitated using the FluorChem program spot densitometry function. A: Representative clearance curves. B: Averaged AUC peptide plasma concentrations (n = 3 for all conditions). No significant differences.

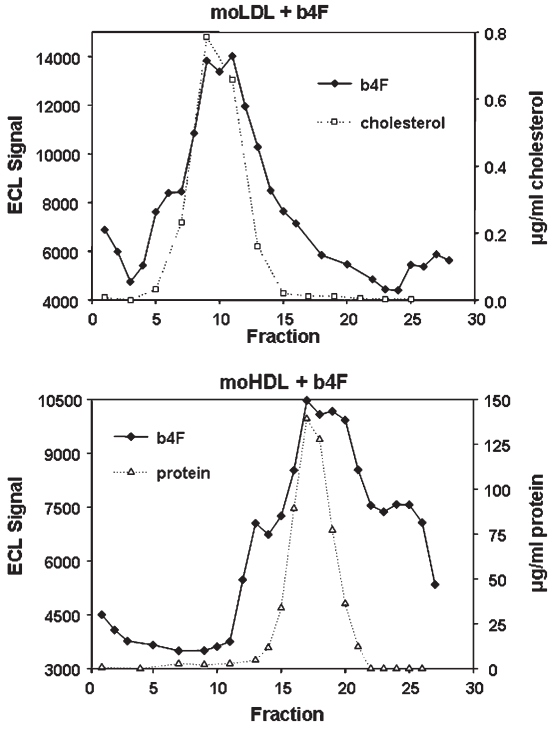

Fig. 2. In vitro b4F-lipoprotein association assays. moLDL or moHDL (400 µg, by protein) was incubated with 117 µg peptide and separated by 3–20% NaBr ultracentrifugation gradient. Density fractions were applied to Immobilon in a slot-blot apparatus and the membrane was probed with avidin-HRP. The blot was quantitated using the FluorChem program spot densitometry function. The lipoprotein distribution was followed by total protein (HDL) or TC (LDL).

by protein content (Fig. 2). Therefore, it can be stated that in the absence of competing binding substrates, b4F can associate with moLDL and moHDL in vitro, but not that either lipoprotein is strongly or preferentially bound.

In vivo administration of biotinylated peptides demonstrates HDL binding by bPro but not b4F

In vitro experiments provided a potential mechanism for the lack of correlation between b4F plasma clearance and plasma HDL concentration: b4F can interact with both LDL and HDL. We investigated this possibility in vivo by injecting mice IP with 300 µg of b4F or bPro. Based on our peptide plasma clearance results, we chose to exsanguinate the mice 2 h postinjection, a time at which the peptides were approaching their plasma concentration peak (Fig. 1; data not shown). In addition to providing a robust signal, the 2 h time point avoided the cumulative effects of lipoprotein metabolism that might confound inference of the initial lipoprotein association behavior of the peptides.

Equal amounts of mouse plasma obtained 2 h postinjection were separated by FPLC and the fractions probed for b4F with avidin-HRP. When b4F was injected into wild-type C57 mice (**Fig. 3A**), the highest peptide signal peak was fraction 52. The identification of cholesterol and apoA-I peaks at fraction 49-50 indicates that the b4F peak at fraction 52 corresponds with "late HDL" as described by Navab et al. (2). Post-HDL fractions contain plasma free protein, the great majority of which is albumin, beginning at fraction ~54 (see protein signal in bPro graph in Fig. 3A). The b4F peak at fraction 52 therefore represents a post-HDL, prealbumin fraction. There was also a large b4F signal peak at fraction 38. This peak was also present in b4F-treated apoE$^{-/-}$ (Fig. 3B) and apoE$^{-/-}$apoA-I$^{-/-}$ mice (Fig. 3C). However, very little cholesterol was detected in these fractions. Following centrifugation of pooled FPLC fractions 34-40 from apoE$^{-/-}$ mice on density gradients, the b4F signal was in the bottom fraction (data not shown), consistent with the peptide signal in these fractions not representing lipoprotein association but rather association with a protein complex.

bPro injected into wild-type C57 mice showed a much different pattern (Fig. 3A). Discrete peptide signal peaks corresponded to chylomicron remnants/VLDL (fraction 10), LDL (fraction 28), early HDL (fraction 42), and HDL (fraction 48). There was no peak corresponding to late HDL (i.e. post-HDL, prealbumin fractions) as was the case for b4F.

When b4F was injected into apoE$^{-/-}$ mice (Fig. 3B), three peaks of peptide signal were apparent: chylomicron remnants/VLDL (fraction 12), the nonlipoprotein peak at fraction 36, and the late HDL peak. The latter two peaks had both been seen in b4F-treated wild-type C57 mice (Fig. 3A). The appearance of the chylomicron remnant/

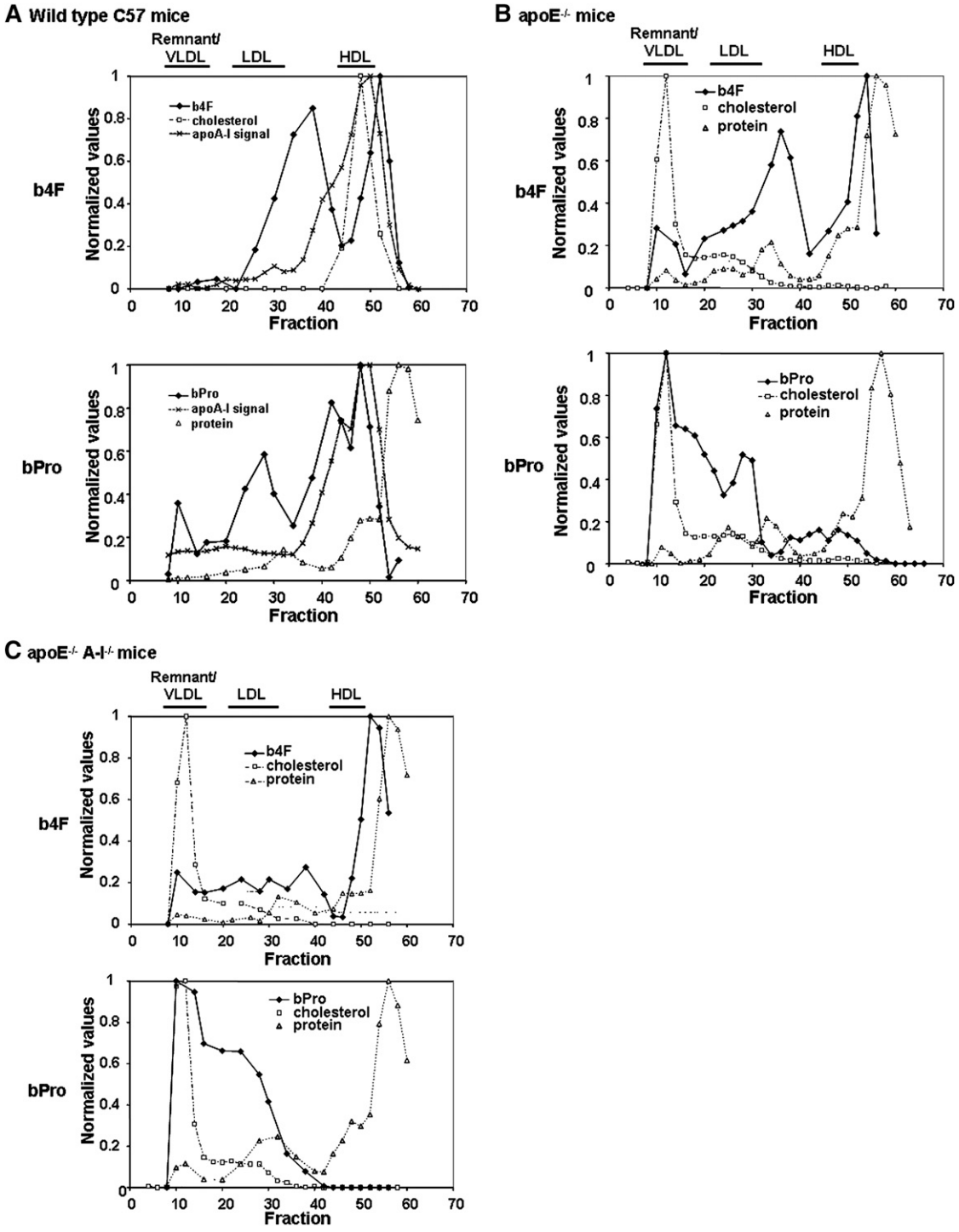

Fig. 3. Representative FPLC curves from in vivo biotinylated peptide lipoprotein-association experiments. A: Wild-type C57 mice, B: apoE$^{-/-}$ mice, and C: apoE$^{-/-}$apoA-I$^{-/-}$ mice were injected IP with 300 μg of either b4F, bPro, or PBS. After 2 h, mice were bled and equal amounts of plasma were separated by FPLC. FPLC fractions of a peptide-treated mouse were applied to Immobilon membrane in a slot blot apparatus along with FPLC fractions from a PBS-treated mouse. The avidin-HRP signal of the control mouse FPLC fractions was subtracted from that of the peptide-treated mouse to ensure representation of peptide-specific signal. The membrane was reprobed for apoA-I and the FPLC fractions were assayed for cholesterol and/or protein content as described in "Methods." All experiments were performed at least twice; representative curves are shown.

VLDL peak corresponds to the elevated level of this lipoprotein population in the apoE$^{-/-}$ mice.

bPro injected in apoE$^{-/-}$ mice showed a number of peptide signal peaks (Fig. 3B). The highest peak was for chylomicron remnants/VLDL, with a strong tailing signal into IDL/LDL. Peaks were also present for early HDL (fraction 44) and mature HDL (fraction 48). Once again, there was no appreciable bPro signal peak in the late HDL (fraction 52). Therefore, the bPro signal traces are very similar in C57 and apoE$^{-/-}$ mice, with the differences in

the relative heights of the peptide signal peaks likely due to differences in relative lipoprotein concentrations in these mice.

Finally, the biotinylated peptides were injected into HDL-less apoE$^{-/-}$apoA-I$^{-/-}$ mice (Fig. 3C). b4F showed only one strong peak, which occurred at fraction 51. This fraction represents late HDL in HDL-sufficient plasma; however, because apoE$^{-/-}$apoA-I$^{-/-}$ mice do not contain HDL, this demonstrates that b4F does not actually bind to late HDL but rather to a plasma protein or complex that also elutes in that fraction. This observation was confirmed in ex vivo experiments (data not shown), i.e. the preservation of the b4F late HDL signal in the plasma from HDL-less mice.

In apoE$^{-/-}$apoA-I$^{-/-}$ mice, bPro showed a very similar trace to that from apoE$^{-/-}$ mice except for a complete lack of signal in the HDL range (Fig. 3C). The bPro signal peaked at chylomicron remnants/VLDL with a strong tail into IDL/LDL and late LDL. Importantly, the HDL signal that was present in bPro-treated apoE$^{-/-}$ mice completely disappeared in apoE$^{-/-}$apoA-I$^{-/-}$ mice.

Overall, FPLC traces from in vivo lipoprotein-association experiments (Fig. 3) closely agree with the ultracentrifugation traces of ex vivo experiments (data not shown). bPro associates with all lipoprotein classes present in plasma both ex vivo and in vivo, including a specific mature HDL peak that is abrogated in the absence of HDL (apoE$^{-/-}$apoA-I$^{-/-}$ mice). b4F, on the other hand, associates primarily with late HDL FPLC fractions regardless of the presence or absence of plasma HDL. This behavior generally agrees with what was seen in ex vivo ultracentrifugation experiments. Overall, the in vivo results from Fig. 3 demonstrate that bPro widely associates with all lipoprotein classes and specifically binds HDL. b4F, on the other hand, associates with a nonlipoprotein complex at FPLC fraction 36 and in late HDL size fractions regardless of the presence of plasma HDL.

b4F does not associate with a lipoprotein smaller than LDL in vivo, whereas bPro specifically interacts with HDL

To confirm the lipoprotein nature of the biotin signal peaks in the HDL/late HDL fractions, apoE$^{-/-}$ mouse FPLC fractions that comprised peptide signal peaks were pooled and subjected to density gradient ultracentrifugation followed by immunoblotting with avidin-HRP. Analysis of b4F-treated apoE$^{-/-}$ mouse FPLC fractions 52-56 showed that the vast majority of the b4F signal was present in the bottom of the ultracentrifuge tube (**Fig. 4A**). This was despite the presence of a large apoA-I signal peak in the small HDL density range. Therefore, this ultracentrifugation experiment seems to confirm the non-HDL nature of the late FPLC b4F peak. The null hypothesis would be that b4F associates with small HDL very loosely, an interaction that is disrupted during the density gradient ultracentrifugation. However, taking this result together with the presence of the late HDL b4F peak in apoE$^{-/-}$apoA-I$^{-/-}$ plasma, we conclude that b4F does not bind HDL in plasma.

bPro-treated apoE$^{-/-}$ mouse FPLC fractions 48-52 were similarly subjected to density gradient ultracentrifugation.

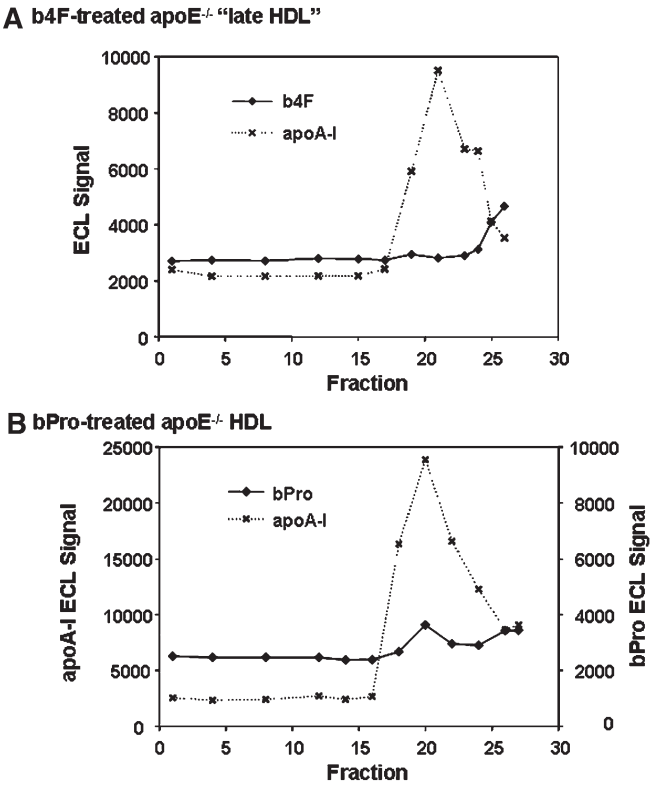

Fig. 4. Density gradient examination of the FPLC fractions corresponding to the HDL/late HDL peptide signal peaks from b4F- or bPro-treated apoE$^{-/-}$ mice. For each HDL population (b4F late HDL fractions 52-56, bPro HDL peak fractions 48-52), FPLC fractions from two replicate in vivo experiments were pooled and the pooled fractions separated on a 3–20% NaBr ultracentrifugation gradient. Density gradient fractions were applied to Immobilon membrane in a slot blot apparatus and probed with avidin-HRP to detect b4F (A) or bPro (B) and reprobed with anti-apoA-I antibody. The ECL signal was quantitated using the spot densitometry function of the FluorChem program. ECL background signal for this exposure time was ~2500.

Slot blotting of the density fractions showed strong apoA-I signal in fractions corresponding to the density of HDL (density gradient fraction 20) (Fig. 4B). Importantly, the bPro signal showed a peak that precisely matched this density. This result confirms that bPro does indeed associate with HDL. In addition, there was peptide signal in the bottom ultracentrifugation fractions, suggesting either peptide falling off during the ultracentrifugation or a population of unbound bPro.

Hb is consistently present in the late HDL fractions corresponding to the b4F peak

Our results demonstrated that b4F was not associating with HDL in the late HDL fractions. This finding contradicts several previous reports of apoA-I mimetic peptide HDL association (2, 6, 7) and it was therefore of great interest to determine what, in fact, b4F did bind in this fraction. To examine this, FPLC fractions representing b4F and bPro peptide signal peaks from in vivo experiments with apoE$^{-/-}$ mice were compared by Coomassie-stained SDS-PAGE (**Fig. 5A**). The late HDL fractions with either peptide (lanes 4 and 10) contain apoA-I,

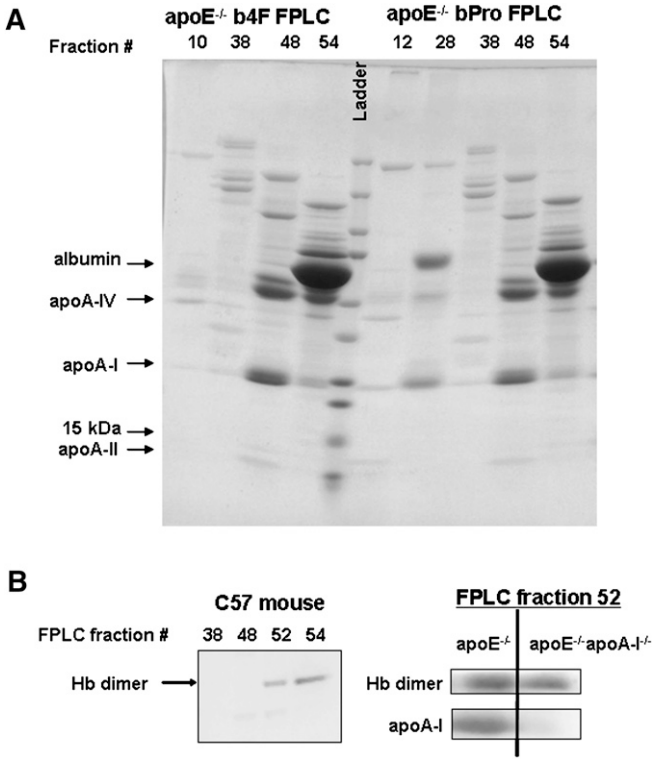

Fig. 5. Comparison of the apoproteins and plasma proteins present in FPLC fractions representing b4F and bPro peaks. A: Coomassie-stained SDS-PAGE of FPLC fractions from b4F- and bPro-treated apoE$^{-/-}$ mice. Arrows indicate the identity of known HDL apoproteins and albumin. The 15 kDa protein is also indicated by an arrow. Protein ladder, from bottom to top: 10, 15, 20, 25, 37, 50, 75, 100, 150, 250 kDa. B: Anti-Hb immunoblots demonstrating the distribution of Hb in FPLC-separated wild-type C57 plasma and the presence of Hb in late HDL fractions of apoE$^{-/-}$ and apoE$^{-/-}$apoA-I$^{-/-}$ plasma.

albumin, and apoA-IV as confirmed by immunoblots (data not shown). There were also variable amounts of protein at ~10–15 kDa.

We hypothesized that the 10–15 kDa protein could represent Hb, given our previous identification of that protein in the late HDL fractions of ultracentrifuged plasma by mass spectrometry (data not shown). Anti-Hb immunoblots were performed on FPLC-isolated HDL and late HDL fractions (Fig. 5B). The polyclonal antibody used for these blots binds both monomeric α- and β-globin (14 kDa) as well as dimeric globin (28 kDa). Late HDL fractions from wild-type C57, apoE$^{-/-}$, and apoE$^{-/-}$apoA-I$^{-/-}$ mice contained significant amounts of dimeric Hb.

We have performed proteomics studies that have demonstrated Hba and Hbb to be present at low levels in FPLC fractions representing mature HDL from wild-type C57 mice (data not shown). However, the ultracentrifugation of these FPLC fractions showed that none of the Hba or Hbb associated with the floating HDL; all globin was found in the free protein ultracentrifugation fractions (data not shown). This result confirms that b4F association with Hb is not dependent on HDL. Overall, we identified four consistent proteins in the late HDL peak of b4F: albumin, apoA-I, apoA-IV, and Hb.

b4F and bPro show opposite binding responses to moHDL

SPR allows sensitive determination of the binding between a ligand and an analyte. The biotin moiety on the N terminus of the b4F and bPro peptides allows extremely avid directional binding of the peptide to the streptavidin BIAcore chip, with the helical portion of the peptide oriented away from the chip to allow native binding conditions with analytes. A recent report has described that b4F and acetylated 4F behave identically in SPR experiments (17).

We first investigated the binding properties of the peptides for moHDL. Given our findings from ex vivo and in vivo lipoprotein experiments, we expected that bPro would show affinity binding for moHDL while b4F would not. Flowing the same sample of moHDL over b4F- and bPro-containing flow cells simultaneously showed detectable binding by bPro but none by b4F (**Fig. 6A**). bPro response to moHDL increased with time without a plateau over 300 s and that binding is competed by nonbiotinylated Pro peptide (Fig. 6B). On the other hand, b4F showed no increase in RU during the moHDL association phase (Fig. 6A). This result provided a confirmation of our in vivo lipoprotein association studies that b4F does not show strong affinity for moHDL. While b4F did associate with purified moHDL in an ex vivo study (Fig. 2) as well as in moHDL remodeling experiments (3), those were endpoint, not kinetic, assays that lacked any competitors. Without any competition, it appears that b4F/4F can associate with moHDL without a strong binding affinity.

The number of amphipathic α-helices and their linker influences the anti-inflammatory effects of apoA-I mimetic peptides in vivo

Having defined the lipoprotein-association profile of b4F and bPro, we next studied the in vivo effects of short-term administration of acetylated peptides to dyslipidemic chow-fed apoE$^{-/-}$ mice. Peptides were acetylated in place of the biotin residue to increase their apoA-I mimicking properties, as shown by others (8), and to coincide with the peptides used in previous investigations by ourselves and others (2, 3).

The studies of Navab et al. (2) have shown that oxidative and inflammatory markers correlate with peptide anti-atherogenicity. We investigated the ability of tandem peptides Pro and Ala (4F-Ala-4F), relative to 4F, to modify plasma lipid and lipoprotein levels, create more plasma preβ-HDL, reduce levels of the plasma inflammatory marker SAA, reduce plasma oxidation, and modify serum PON1 arylesterase activity in apoE$^{-/-}$ mice. The Ala peptide was included to determine if differences in peptide effects were due to the addition of the tandem helix or to the linking proline residue.

Explanations for the beneficial physiologic effects of 4F have focused on HDL binding and the influence of peptide on HDL antioxidative and anti-inflammatory effects. Given the identification of bPro as an HDL binding peptide and b4F as a nonbinding peptide, the effects of these peptides when administered to dyslipidemic mice could

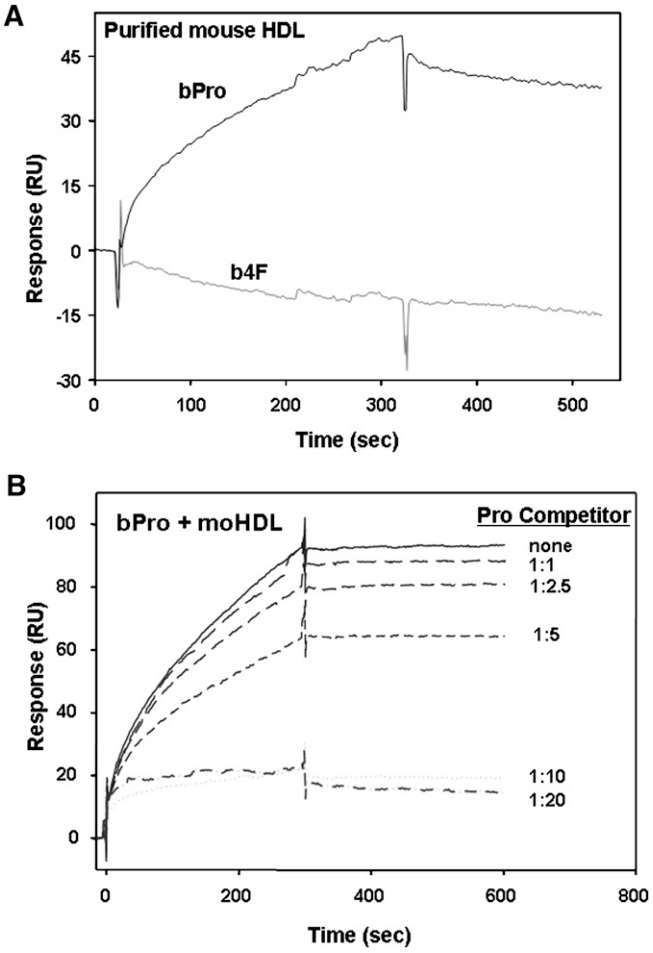

Fig. 6. SPR binding of biotinylated peptides to moHDL. b4F and bPro were deposited on separate flow wells of a streptavidin-linked SPR chip, generating approximately equal levels of RU. A: 100 nM moHDL (analyte) flowed over both of the peptides during one representative run, allowing simultaneous monitoring of the binding response to both peptides. The response to both the analyte association and dissociation phase is displayed (300 s for each). B: Competitive binding assay of bPro for moHDL. A total of 200 nM moHDL (analyte) was flowed over the bPro either alone or in the presence of increasing concentrations of competitor Pro (unbiotinylated acetylated peptide). The response to both the analyte association and dissociation phase is displayed (300 s for each).

be different. However, bPro and b4F could provide similar results while working via different mechanisms. Whereas bPro binds HDL, b4F coelutes with Hb and could act as an antioxidant scavenger for the small physiologic amounts of proinflammatory free Hb (18, 19).

Peptides were administered IP to 8-to 10-week-old female mice with similar total plasma cholesterol (TC) levels at equal molar doses, which provided roughly equal bioavailability across peptides based on head-to-head biotinylated peptide clearance experiments (data not shown). The peptides were administered every other day for 1 week for a total of three injections. 4F was administered at 50 μg, while Pro and Ala were administered at 100 μg. The 4F peptide dose is more than twice as much peptide (50 vs. 20 μg) half as often (every 48 h vs. every 24 h) compared with the protocol used in the Garber et al. (7) study of the 5F peptide. Our dosage schedule had larger peaks and troughs than every day IP administration, but lowered the total number of traumatic injections and is predicted to have a roughly equal AUC compared with a daily injection of one-half as much peptide.

Mice were euthanized 2 h after the last injection to sample the plasma at roughly the height of peptide concentration. There were no significant differences in body weight or plasma TBARS between animals given PBS injection and those receiving any peptide (**Table 1**). We expected that short-term peptide treatment would be sufficient to decrease plasma oxidative markers, based on previous work with D4F (20, 21). However, TBARS is a crude test of malondialdehyde, which is a late oxidative epitope.

We also measured the baseline plasma cholesterol and the plasma cholesterol and lipoprotein distribution after peptide treatment (**Table 2**). No differences were observed after treatment with 4F or either tandem peptide compared with PBS-treated controls. This is in agreement with the finding of Navab et al. (20), who did not describe any lipid changes due to D4F treatment. However, a previous report showed IP administration of 5F for 8 weeks significantly decreased plasma HDL-C despite having antiatherogenic effects (7). There were no apparent differences in the FPLC cholesterol trace after any peptide treatment compared with PBS-treated mice (data not shown), demonstrating no detectable effect of 1 week of peptide treatment on lipoprotein remodeling or metabolism. Longer term treatment could be necessary to influence lipoprotein metabolism.

Navab et al. (21) have described that D4F increased lipid-poor preβ HDL in the face of unchanged HDL-C levels. Therefore, we tested whether our peptide treatments influenced the agarose gel migration pattern of plasma apoA-I. We expected tandem peptides Pro and Ala, which more readily displaced apoA-I from HDL in vitro (3), to form more preβ HDL compared with monomeric 4F. However, we saw very little signal in the preβ migratory position, regardless of peptide treatment (**Fig. 7**). Given our results from Fig. 1, 300 μg b4F injected IP achieved ~54 μM peak blood concentration. We injected one-third of this dose for the tandem peptides and one-sixth of this dose for 4F. Assuming clearance is not affected by this dose reduction, we would still be in the peptide concentration range where we observed HDL remodeling in our in vitro experiment (3). Given those assumptions, the most likely explanation is that the presence of other lipoproteins and plasma proteins moderate peptide remodeling activity.

TABLE 1. Effect of short-term peptide treatment of apoE$^{-/-}$ mice on body weight and plasma oxidation

Peptide Treatment	Weight (g)	Plasma TBARS (pmol TEP equivalent/μl plasma)
PBS	16.7 ± 1.2	4.92 ± 1.96
4F	17.6 ± 0.9	5.88 ± 2.21
Pro	17.8 ± 1.7	5.59 ± 1.37
Ala	16.6 ± 1.4	5.99 ± 2.4

n = 4, average ± SD. No significant differences.

TABLE 2. Effect of short-term peptide treatment of apoE$^{-/-}$ mice on plasma TC and lipoprotein levels

Peptide Treatment	Prebleed TC (mg/dl)	Final TC (mg/dl)	Chylomicron Remnants/ VLDL-C(mg/dl)	LDL-C (mg/dl)	HDL-C (mg/dl)
PBS	386 ± 81	512 ± 133	341 ± 105	152 ± 42	18 ± 7
4F	387 ± 27	574 ± 63	393 ± 71	164 ± 34	16 ± 7
Pro	373 ± 50	545 ± 57	386 ± 47	146 ± 34	13 ± 7
Ala	337 ± 65	550 ± 98	377 ± 80	164 ± 25	10 ± 8

n = 4, average ± SD. No significant differences.

apoE$^{-/-}$ mice also have a band of apoA-I signal between the α and preβ migratory positions, which was not affected by peptide treatment (Fig. 7). The identity of this band is unknown.

PON1 is an important plasma antioxidative enzyme that can associate with HDL. In previous reports, administration of D4F in vivo or ex vivo shifted serum PON1 activity into late HDL fractions and increased total serum activity (2, 21). We assessed total serum PON arylesterase activity in peptide-treated mice and saw no difference in any treatment group (**Fig. 8A**). The distribution of PON1 activity in EDTA-free FPLC fractions has been described for a variety of mouse models (13). In apoE$^{-/-}$ mice, a large proportion of the PON arylesterase activity (Fig. 8B) as well as PON1 protein (data not shown) is found in post-HDL fractions. Comparing the distribution of PON activity in PBS- or 4F-treated apoE$^{-/-}$ mice showed no significant changes in HDL-associated activity in 4F-treated apoE$^{-/-}$ mice (data not shown).

SAA is an acute-phase reactant produced by the liver in response to innate immune cytokines (interleukin-1, tumor necrosis factor-α, and interleukin-6) (22). Plasma SAA is predominately HDL-associated. Cholesterol-fed rabbits show elevated plasma SAA levels, which were significantly reduced by subcutaneous injections of 4F or D4F (23). However, another report showed no difference in plasma SAA in 20-week-old high-cholesterol/high-fat diet-fed apoE$^{-/-}$ mice after 4 weeks of oral or IP D4F treatment compared with saline control mice (24).

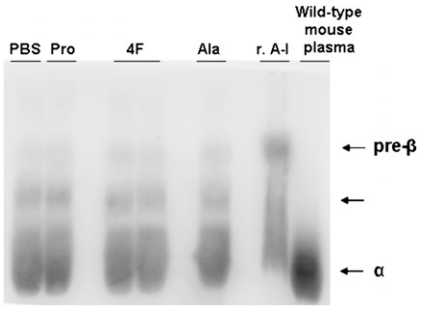

Fig. 7. Agarose gel separation of plasma from short-term peptide-treated apoE$^{-/-}$ females. Total mouse plasma was separated on a 0.7% agarose gel (25 mM Tricine/3 mM calcium lactate) along with recombinant apoA-I (r. A-I). The gel was then transferred to Immobilon and probed with a polyclonal antibody against mouse apoA-I. Migratory positions (alpha, pre-beta, and unidentified) are denoted by arrows.

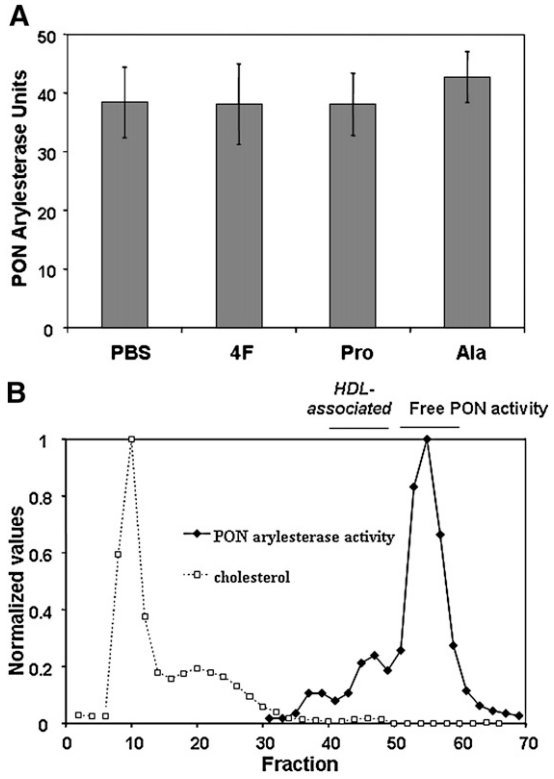

Fig. 8. Neither total serum PON1 arylesterase activity nor its distribution in FPLC fractionated serum is modified by short-term peptide treatment in apoE$^{-/-}$ mice. A: Serum PON arylesterase activity. The arylesterase activity of six concentrations of unfractionated serum was determined for each mouse as described in "Methods" to determine specific activity. The average serum PON specific activity of each peptide treatment group was determined with an n = 4 mice per group; no significant differences were observed. B: Representative FPLC (EDTA-free buffer) of apoE$^{-/-}$ serum demonstrating PON1 arylesterase activity.

We assessed SAA levels by immunoblotting plasma separated on SDS-polyacrylamide gels with a polyclonal antibody against all mouse SAA isoforms (**Fig. 9A**). Only Pro treatment showed a significant decrease in SAA signal compared with PBS-treated mice. Quantitation of immunoblots from three independent experiments demonstrated the Pro treatment effect to be reproducible and significant (Fig. 9B). Plasma apoA-I concentration was not modified by peptide treatment (Fig. 9C). These results demonstrate an anti-inflammatory effect of short-term Pro, but not 4F, treatment in apoE$^{-/-}$ mice under these experimental conditions.

DISCUSSION

We have examined the plasma clearance rates and lipoprotein association properties of two peptides, b4F and bPro. b4F and bPro show significant differences in protein/lipoprotein association, which are summarized in **Table 3**. We also analyzed plasma cholesterol, plasma TBARS, serum PON arylesterase activity, and plasma SAA expression in peptide-treated mice as a measure of the antioxidative and anti-inflammatory action of the peptides.

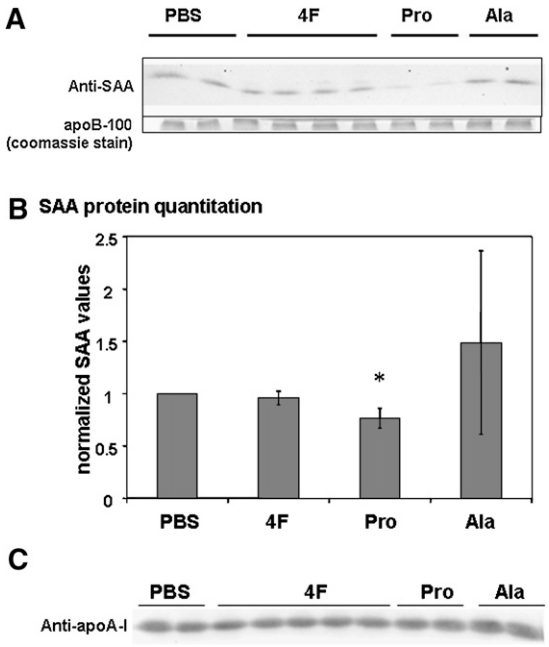

Fig. 9. Short-term treatment with the Pro peptide significantly decreases plasma SAA, but not apoA-I, levels. A: Representative anti-SAA immunoblot of whole plasma. Coomassie stained protein at the apoB-100 position is included as a loading control. B: Normalized spot densimetric quantitation of SAA immunoblots. n = 3, * = $P < 0.007$ versus PBS. No other significant changes. C: Representative anti-apoA-I immunoblot of whole plasma.

Several of these studies were performed in different mouse strains (C57 wild-type, apoE$^{-/-}$, and apoE$^{-/-}$apoA-I$^{-/-}$), which differed in HDL status.

All plasma clearance and lipoprotein-association experiments were performed with biotinylated peptides. By using a biotin tag, we were able to assess the plasma clearance of b4F in three mouse models with varying amounts of plasma HDL. Given the work by Navab et al., we expected the b4F clearance curves to be governed by the plasma HDL status. This was not the case; no significant differences in b4F clearance were seen among wild-type C57, apoE$^{-/-}$, or apoE$^{-/-}$apoA-I$^{-/-}$ mice. These mice have high levels, low levels, and undetectable levels of HDL, respectively.

Given this completely unexpected result, we assessed the ability of b4F to bind lipoproteins in vitro. b4F showed no deficit in binding isolated moLDL or moHDL. To confirm this result in a more physiological environment, we performed in vivo lipoprotein-association studies. Taking all b4F association experiments together, b4F generally showed its highest peak in those fractions that represent small dense HDL, or late HDL. This was the case even in the HDL-deficient apoE$^{-/-}$apoA-I$^{-/-}$ mouse. We have identified Hbα and β in the late HDL fractions under several experimental conditions (regardless of HDL status). The suggestion of Hb as a potential b4F binding partner was completely unexpected. We are cognizant that this result could be confounded by hemolysis. All bleeds for these experiments showed clear-to-yellow plasma without visibly detectable hemolysis. However, even good blood collection technique is associated with plasma Hb concentrations of 9–120 mg/L (25). The presence of small amounts of Hb in plasma, given potential affinity binding of b4F to Hb, could be skewing the results away from the true in vivo situation. We can likely exclude peptide-mediated hemolysis (26) as the basis for these results, as b4F associates with Hb-containing fractions in late HDL fractions even in ex vivo plasma-based experiments with apoE$^{-/-}$ or apoE$^{-/-}$apoA-I$^{-/-}$ plasma (data not shown). The basis of the Hb-b4F association is not due to biotin binding, as bPro does not show the same behavior. The 4F helix does not have homology with any proteins expected to bind Hb.

Given its short size and lack of potential curvature, we expected the b4F peptide to associate with HDL as well as other plasma lipoproteins such as chylomicron remnants/VLDL. Association of b4F with chylomicron remnants/VLDL was variable between experiments and never showed a large signal peak. This result suggests the peptide's ability to interact with these large lipoproteins is not as great as we hypothesized.

Previous work on the antiatherogenic mechanism of action of 4F suggests that the peptide must interact with HDL, resulting in the acquisition of lipoperoxides from the holoparticle and HDL remodeling to generate preβ HDL. We show that 4F has the capacity to bind when presented to isolated HDL, separate from other lipoproteins and plasma components that operate as potential competitors in vivo. Our results suggest that the 4F-HDL interaction is low affinity and involves relatively rapid on and off kinetic behavior. No investigator has demonstrated a high affinity of 4F for HDL and previous reports of D4F/5F-HDL association were based upon plasma equilibrium results that simply inferred that a late FPLC peptide signal peak was due to HDL binding without testing for a specific association. Further work with the HDL-less mice will help

TABLE 3. Summary of the lipoprotein-association properties of biotinylated peptides

		Peptide Used	
Experiment	Ligand	b4F	bPro
Centrifuge-based in vitro association assays	moHDL	+	N/A
	moLDL	+	N/A
SPR	moHDL	•	+
In vivo plasma association (FPLC-based)	C57 wild-type mice	Late LDL and late HDL fractions	All lipoproteins
	apoE$^{-/-}$ mice	Late LDL and late HDL fractions	All lipoproteins
	apoE$^{-/-}$/apoA-I$^{-/-}$ mice	Late HDL fractions	All lipoproteins, no peak in HDL fractions

Symbols for assays with purified ligand: •, no binding; +, binding; not assayed = N/A.

to ascertain whether this interaction is important for the in vivo bioactivity of the 4F peptide. While we cannot conclusively eliminate the effect of biotinylation on peptide distribution characteristics, we believe that the evidence in toto does not support that modification being a significant caveat for our work.

Taking all bPro association experiments together, the tandem peptide consistently associated with all lipoprotein classes. This included the mature HDL fractions, which were specific for plasma HDL status. bPro specifically associates with moHDL in SPR experiments and that binding can be competed with acetylated Pro (Fig. 6). Our original hypothesis was that the presence of a proline linker would bias the Pro peptide to binding small lipoproteins. However, the presence of bPro in the chylomicron remnant/VLDL fractions is not consistent with this hypothesis. The behavior of only one labeled tandem peptide was tested, so the differences of bPro versus b4F cannot be conclusively said to be due to the presence of the proline linker. The behavioral change could also be due to the effect of doubling the helix number.

We hypothesized that the Pro peptide better modeled lipid-associated full-length apoA-I because of its tandem helices separated by a proline kink. However, neither b4F nor bPro associated with plasma lipoproteins in a manner analogous to apoA-I. Other studies have shown that lipid-free apoA-I injected into wild-type rabbits or mice rapidly associated with preexisting α mobility particles (7, 27). The b4F peptide does not actually associate with HDL, while bPro associates with all lipoprotein classes, including HDL. Obviously, the proline kink does not provide the expected biophysical barrier to association of the Pro peptide with large lipoproteins. Potential reasons for this unexpected result include, but are not limited to: *1*) the tandem Pro peptide could be interacting with large lipoproteins with only one helix, thereby bypassing the effects of the proline residue, or *2*) in the very α-helical environment of tandem 4F helices, the proline residue could function as a more flexible linker than is suggested from the isolated structural studies.

Short-term IP administration of equimolar amounts of mimetic peptides to young apoE$^{-/-}$ mice generally showed little effect on measured plasma parameters (Tables 1, 2). No changes were observed in body weight, plasma TBARS, total plasma cholesterol, lipoprotein profile, preβ migrating HDL, serum PON activity, or PON lipoprotein distribution. This experiment used an IP peptide dose roughly equal to that of the similarly designed long-term 5F atherosclerosis study by Garber et al. (7). That study did not observe HDL remodeling while observing significantly decreased HDL-C, but they did report significantly decreased HDL lipid hydroperoxides. Oral D4F shows highly potent anti-inflammatory and antioxidative effects (20, 21) despite very low bioavailability. The reason(s) our peptides do not show the same efficacy as these previous reports is unknown. It is possible that the IP route of peptide administration affected the efficacy of our peptides, though we consider this unlikely given the results of Garber et al. (7). However, we were able to observe a significant decrease in the plasma SAA level in Pro-treated mice. We do not believe that this difference of SAA effect between peptides is due to differential clearance, based on head-to-head plasma clearance studies using biotinylated peptides (data not shown) and the fact that both peptides are <5,000 Da and are therefore both likely to be readily cleared by the kidneys (28).

In sum, the peptides in our hands seem to show some anti-inflammatory ability in apoE$^{-/-}$ mice. Peptide-mediated HDL remodeling or antioxidative ability was not observed in vivo. This was despite readily observable in vitro effects on these parameters (3). The observations reported here provide a platform for interpreting the results of long-term administration of peptide to atherosclerosis-prone mice.

The authors thank Dr. Timothy Sontag for the recombinant mouse apoA-I protein, wild-type mouse plasma lipid measurements, and valuable scientific discussions. Dr. Elena Solomaha provided training and advice for the SPR experiments.

REFERENCES

1. Anantharamaiah, G. M., V. K. Mishra, D. W. Garber, G. Datta, S. P. Handattu, M. N. Palgunachari, M. Chaddha, M. Navab, S. T. Reddy, J. P. Segrest, et al. 2007. Structural requirements for antioxidative and anti-inflammatory properties of apolipoprotein A-I mimetic peptides. *J. Lipid Res.* **48:** 1915–1923.
2. Navab, M., G. M. Anantharamaiah, S. T. Reddy, S. Hama, G. Hough, V. R. Grijalva, N. Yu, B. J. Ansell, G. Datta, D. W. Garber, et al. 2005. Apolipoprotein A-I mimetic peptides. *Arterioscler. Thromb. Vasc. Biol.* **25:** 1325–1331.
3. Wool, G. D., C. A. Reardon, and G. S. Getz. 2008. Apolipoprotein A-I mimetic peptide helix number and helix linker influence potentially anti-atherogenic properties. *J. Lipid Res.* **49:** 1268–1283.
4. Sankararamakrishnan, R., and S. Vishveshwara. 1990. Conformational studies on peptides with proline in the right-handed alpha-helical region. *Biopolymers.* **30:** 287–298.
5. Barlow, D. J., and J. M. Thornton. 1988. Helix geometry in proteins. *J. Mol. Biol.* **201:** 601–619.
6. Garber, D. W., Y. V. Venkatachalapathi, K. B. Gupta, J. Ibdah, M. C. Phillips, J. B. Hazelrig, J. P. Segrest, and G. M. Anantharamaiah. 1992. Turnover of synthetic class A amphipathic peptide analogues of exchangeable apolipoproteins in rats. Correlation with physical properties. *Arterioscler. Thromb.* **12:** 886–894.
7. Garber, D. W., G. Datta, M. Chaddha, M. N. Palgunachari, S. Y. Hama, M. Navab, A. M. Fogelman, J. P. Segrest, and G. M. Anantharamaiah. 2001. A new synthetic class A amphipathic peptide analogue protects mice from diet-induced atherosclerosis. *J. Lipid Res.* **42:** 545–552.
8. Venkatachalapathi, Y. V., M. C. Phillips, R. M. Epand, R. F. Epand, E. M. Tytler, J. P. Segrest, and G. M. Anantharamaiah. 1993. Effect of end group blockage on the properties of a class A amphipathic helical peptide. *Proteins.* **15:** 349–359.
9. Cabana, V. G., J. N. Siegel, and S. M. Sabesin. 1989. Effects of the acute phase response on the concentration and density distribution of plasma lipids and apolipoproteins. *J. Lipid Res.* **30:** 39–49.
10. Reardon, C. A., L. Blachowicz, T. White, V. Cabana, Y. Wang, J. Lukens, J. Bluestone, and G. S. Getz. 2001. Effect of immune deficiency on lipoproteins and atherosclerosis in male apolipoprotein E-deficient mice. *Arterioscler. Thromb. Vasc. Biol.* **21:** 1011–1016.
11. Maliwal, B. P., and F. E. Guthrie. 1982. In vitro uptake and transfer of chlorinated hydrocarbons among human lipoproteins. *J. Lipid Res.* **23:** 474–479.
12. Fisher, W. R., M. G. Hammond, M. C. Mengel, and G. L. Warmke. 1975. A genetic determinant of the phenotypic variance of the molecular weight of low density lipoprotein. *Proc. Natl. Acad. Sci. USA.* **72:** 2347–2351.

13. Cabana, V. G., C. A. Reardon, N. Feng, S. Neath, J. Lukens, and G. S. Getz. 2003. Serum paraoxonase: effect of the apolipoprotein composition of HDL and the acute phase response. *J. Lipid Res.* **44:** 780–792.
14. Lapenna, D., G. Ciofani, S. D. Pierdomenico, M. A. Giamberardino, and F. Cuccurullo. 2001. Reaction conditions affecting the relationship between thiobarbituric acid reactivity and lipid peroxides in human plasma. *Free Radic. Biol. Med.* **31:** 331–335.
15. Aviram, M., and J. Vaya. 2001. Markers for low-density lipoprotein oxidation. *Methods Enzymol.* **335:** 244–256.
16. Jiao, S., T. G. Cole, R. T. Kitchens, B. Pfleger, and G. Schonfeld. 1990. Genetic heterogeneity of lipoproteins in inbred strains of mice: analysis by gel-permeation chromatography. *Metabolism.* **39:** 155–160.
17. Van Lenten, B. J., A. C. Wagner, C-L. Jung, P. Ruchala, A. J. Waring, R. I. Lehrer, A. D. Watson, S. Hama, M. Navab, G. M. Anantharamaiah, et al. 2008. Anti-inflammatory apoA-I-mimetic peptides bind oxidized lipids with much higher affinity than human apoA-I. *J. Lipid Res.* **49:** 2302–2311.
18. Zhang, R., L. Barker, D. Pinchev, J. Marshall, M. Rasamoelisolo, C. Smith, P. Kupchak, I. Kireeva, L. Ingratta, and G. Jackowski. 2004. Mining biomarkers in human sera using proteomic tools. *Proteomics.* **4:** 244–256.
19. Rother, R. P., L. Bell, P. Hillmen, and M. T. Gladwin. 2005. The clinical sequelae of intravascular hemolysis and extracellular plasma hemoglobin: a novel mechanism of human disease. *JAMA.* **293:** 1653–1662.
20. Navab, M., G. M. Anantharamaiah, S. Hama, D. W. Garber, M. Chaddha, G. Hough, R. Lallone, and A. M. Fogelman. 2002. Oral administration of an Apo A-I mimetic Peptide synthesized from D-amino acids dramatically reduces atherosclerosis in mice independent of plasma cholesterol. *Circulation.* **105:** 290–292.
21. Navab, M., G. M. Anantharamaiah, S. T. Reddy, S. Hama, G. Hough, V. R. Grijalva, A. C. Wagner, J. S. Frank, G. Datta, D. Garber, et al. 2004. Oral D-4F causes formation of pre-beta high-density lipoprotein and improves high-density lipoprotein-mediated cholesterol efflux and reverse cholesterol transport from macrophages in apolipoprotein E-null mice. *Circulation.* **109:** 3215–3220.
22. Wool, G. D., and C. A. Reardon. 2007. The influence of acute phase proteins on murine atherosclerosis. *Curr. Drug Targets.* **8:** 1203–1214.
23. Van Lenten, B. J., A. C. Wagner, M. Navab, G. M. Anantharamaiah, S. Hama, S. T. Reddy, and A. M. Fogelman. 2007. Lipoprotein inflammatory properties and serum amyloid A levels but not cholesterol levels predict lesion area in cholesterol-fed rabbits. *J. Lipid Res.* **48:** 2344–2353.
24. Li, X., K. Y. Chyu, J. R. Faria Neto, J. Yano, N. Nathwani, C. Ferreira, P. C. Dimayuga, B. Cercek, S. Kaul, and P. K. Shah. 2004. Differential effects of apolipoprotein A-I-mimetic peptide on evolving and established atherosclerosis in apolipoprotein E-null mice. *Circulation.* **110:** 1701–1705.
25. Copeland, B. E., P. J. Dyer, and A. J. Pesce. 1989. Hemoglobin by first derivative spectrophotometry: extent of hemolysis in plasma and serum collected in vacuum container devices. *Ann. Clin. Lab. Sci.* **19:** 383–388.
26. Sethi AA, JA Stonik, SJ Demosky, and AT Remaley. 2006. Abstract 1203: Complexation of an apoA-I mimetic peptide with phospholipid increases ABCA1-specific cholesterol efflux. *Circulation.* **114:**II 225.
27. Kee, P., K. A. Rye, J. L. Taylor, P. H. Barrett, and P. J. Barter. 2002. Metabolism of apoA-I as lipid-free protein or as component of discoidal and spherical reconstituted HDLs: studies in wild-type and hepatic lipase transgenic rabbits. *Arterioscler. Thromb. Vasc. Biol.* **22:** 1912–1917.
28. Maack, T., V. Johnson, S. T. Kau, J. Figueiredo, and D. Sigulem. 1979. Renal filtration, transport, and metabolism of low-molecular-weight proteins: a review. *Kidney Int.* **16:** 251–270.